Analysis of factors affecting the formation of the particle size spectrum and the aerosol optical depth in mid-latitudes of North Atlantic

E.V. Makienko, D.M. Kabanov, R.F. Rakhimov, and S.M. Sakerin

Institute of Atmospheric Optics,
Siberian Branch of the Russian Academy of Sciences, Tomsk

The data on the spectral variability of the aerosol optical depth, measured during the 39th cruise of *Akademik M. Keldysh* research vessel, are used to analyze the formation of the disperse composition of the atmospheric aerosol in mid-latitudes of the Atlantic. The efficiency of exporting the aerosol component from Europe and North America is considered. Characteristic features of the aerosol disperse composition during perturbations of the optical state of the atmosphere over open ocean are studied. Variations of the disperse composition of ocean aerosol in the atmospheric depth upon the intensification of wind are analyzed.

Introduction

Recent investigations[1-3] have shown that, regardless of the homogeneity of the underlying surface and smoothness of the meteorological parameters oscillations, variations of optical and microphysical characteristics of the aerosol component even in the regions of open ocean (far from continents) have noticeable amplitude of oscillations, which are caused by episodic invasion of the air masses enriched with aerosols of different types of continental origin into the region under study.

Based on the data of spectral measurements of the aerosol optical thickness (AOT) of the atmosphere over Atlantic Ocean,[2] parameters of the disperse structure of aerosol component were reconstructed. Some specific features of the mechanism of formation of the elements of its microstructure in different regions have also been studied. The peculiarities of the disperse structure of aerosol component were analyzed using averaged experimental data in each of the selected regions.[1] The cycle of measurements of the spectral transparency of the atmosphere was organized in 1996, in the frameworks of the 39th cruise of the *Akademik M. Keldysh* research vessel on its route from Halifax (North America) to Europe. This enabled us to estimate some specific features of the formation of aerosol component near two continents and over the open ocean in mid-latitudes, and to study the effect of such factors as wind velocity and distance of the measurement site from a continent.

Time series of the measurement results on the AOT at three wavelengths (0.44, 0.638, and 1.06 μm) is shown in Fig. 1*a*, and the wind direction θ during the cruise is shown in Fig. 1*b*. Abscissa in these Figures is the numbers of the specific realization *k* of the spectral dependence $\tau_k(\lambda_i)$ and corresponding values of the meteorological quantities: wind speed

S_w (Fig. 1*c*) and relative humidity *q* (Fig. 1*d*). It is necessary to note that, when moving from North American continent, (realization 1 till 20) the aerosol turbidity of the atmospheric column decreased quite quickly. Analogous, but inverse tendency is observed when approaching the European continent (realizations 130 till 160). Besides, two peaks of the AOT values (30 to 45 and 67 to 83 realizations) are observed at wind directions close to westward. As will be shown below, they are caused by emission of large particles of the coarse aerosol fraction, in the first case, and accumulative fraction in the second case (see Fig. 1*b*). Other realizations have quite low AOT values and characterize the state of the aerosol component over the open ocean, quite far from continents, which is close to the background state (OO background), according to the classification in Ref. 2.

Let us consider some peculiarities of transformation of the aerosol microstructure along the vessel route from Halifax (North America) through near-continental region (NC) to the water area of the open ocean (OO) since 26 until 30 of August 1996. The changes of the spectral dependences of AOT and particle size distribution along the route from North American continent are shown in Fig. 2.

It is seen in Table 1 that the total cross sections S_a and the volume V_a of the particles of accumulative fraction decrease practically by an order of magnitude in passing to the open ocean. Analogous characteristics of the intermediate disperse fraction in this period of measurements remain quite stable. The dynamics of variations of the particle size spectrum of the accumulative aerosol fraction shown separately (Fig. 2*c*) shows that the farther from the continent, the larger becomes the effective radius (from 0.15 to 0.26 μm) of particles $r_{eff} = 0.75\,V/S$ simultaneously with the decrease of the aerosol number density.

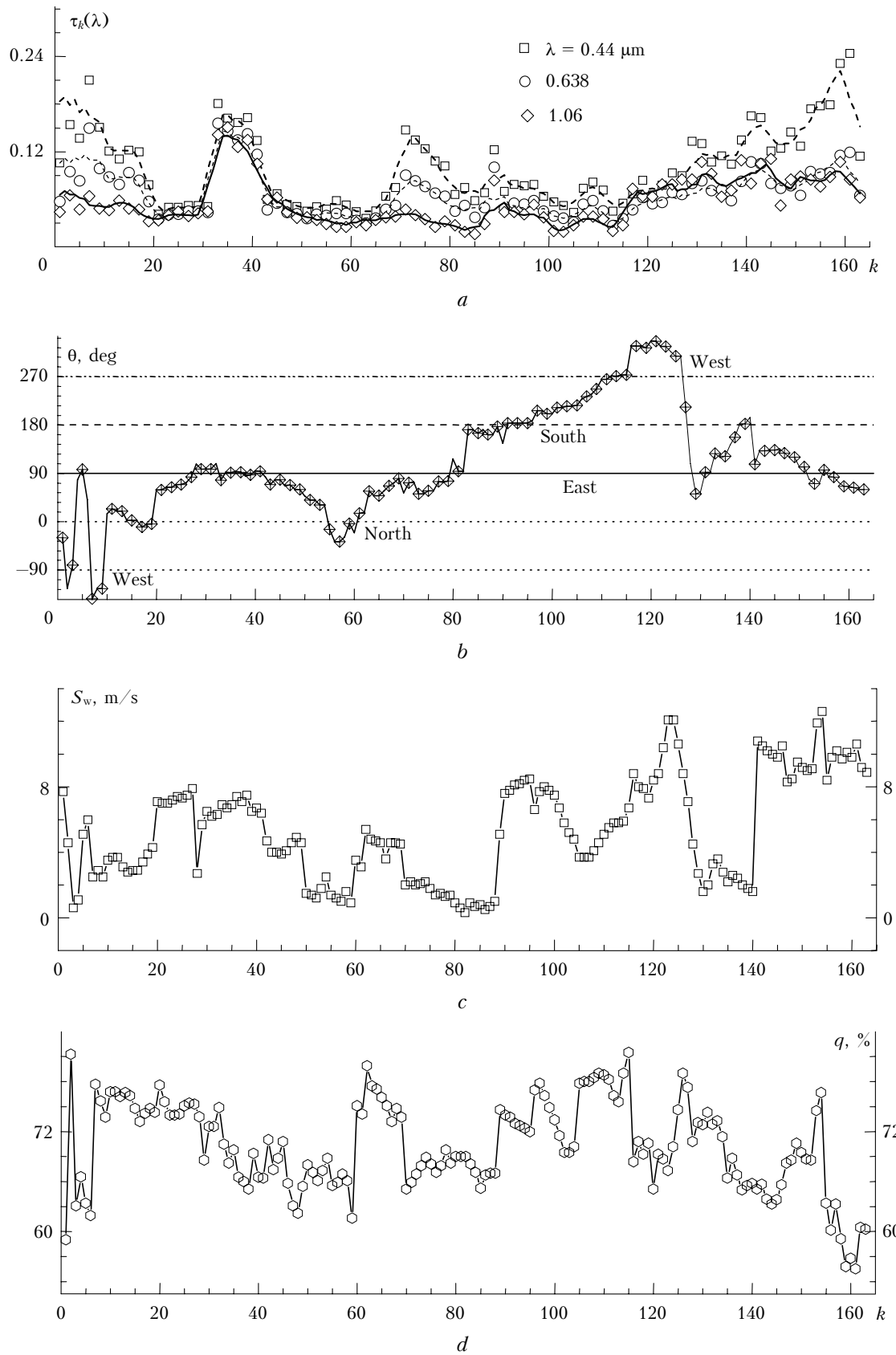　　　　　　　　　© 　2005　Institute　of　Atmospheric　Optics

Fig. 1. Time behavior of AOT measured at the wavelengths of 0.44, 0.638 and 1.06 μm (solid line in Fig. 1*a* shows the smoothed time behavior at the wavelength of 1.06 μm) and meteorological parameters of the atmosphere.

The extreme values of the parameters presented in Table 1 agree with the analogous estimates obtained[2] by inverting the averaged data of many-day measurements of AOT near continent and in the open ocean at the minimum level of the aerosol turbidity of the atmosphere.
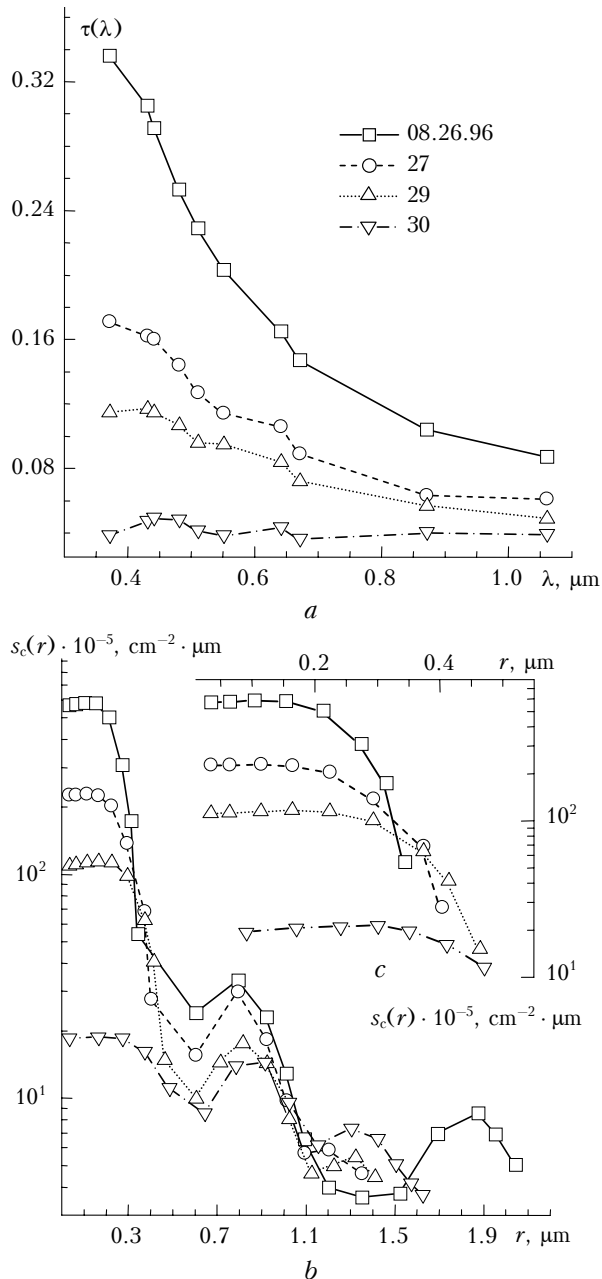

Fig. 2. Daily mean spectra of AOT (*a*), size distributions of geometric cross section $s_c(r)$ (*b*), and the dynamics of accumulative fraction (*c*) in the period of August 26–30, 1996.

Similar tendency of the change of microstructure parameters is observed along the route from OO region to the European continent. It is seen from Fig. 3 that in this case the most essential changes of the aerosol microstructure also occur in the size range

of accumulative fraction, and the characteristics of intermediate size fraction with $r_{eff} \sim 0.8$ μm are approximately at the same level as near the North American continent (Fig. 2*b*).

Table 1. Dynamics of the microstructure parameters of the accumulative aerosol fraction along the route from Halifax into the open ocean

Date	$V_a \cdot 10^{-5}$, μm³ · cm⁻²	$S_a \cdot 10^{-5}$, μm² · cm⁻²	r_{eff}, μm
08.26.96	29	150	0.15
27	16	68	0.17
29	11	41	0.20
30	2.9	8.5	0.26

It follows from the results presented in Figs. 2 and 3 that the effect of continent on the microstructure of the aerosol component is observed at a significant distance from the coast, ~ 500 km and more. In moving from continents, the content of particles of accumulative fraction decreases almost by one order of magnitude. In the open ocean, except for some episodes of the increase of AOT (emission of aerosols from continent), the optical contribution of large particles ($r > 0.45$ μm) undergoes small oscillations and is practically equal and often prevails over the optical effect of the accumulative fraction.

Let us now analyze the aerosol disperse composition (Figs. 4*a* and *b*) reconstructed from the results of observations of AOT (Fig. 4*d*) in the open ocean region (29°N, 43°W) since August 31 until September 2, 1996. During 3 days of the vessel staying during the aforementioned period, approximately triple peak of τ(λ) was observed with subsequent return to the usual values for this region (see realizations 25–45 in Fig. 1*a*). Figure 4*c* shows an example of comparison of the spectral dependence τ(λ) with that calculated from the reconstructed size spectrum (curves *2* in Figs. 4*a* and *b*).

The fact attracts our attention that the peaks of the values τ(λ) coincide in time with the periods when wind direction coincided with the westward transfer of air masses. Analysis of the results presented in Fig. 4 shows that the peak of AOT was caused by invasion of an air mass enriched with particles of all three fractions (accumulative with $r < 0.5$ μm, intermediate dispersed with $0.5 < r < 1.2$ μm, and coarse fraction with $r > 1.2$ μm) to the region of observations. This fact is illustrated by curve *3* calculated as the difference between the volume size spectra reconstructed from the measurement data on September 1 and August 31. Table 2 presents the total volumes and cross sections of three fractions from which the effective size r_{eff} of particles of each fraction have been calculated.

The second analogous peak of atmospheric turbidity was observed at staying of the vessel since September 4 until 6, 1996 (see realizations 67–83 in Figs. 1*a* and *b*). However, the dramatic increase of the content of particles of only accumulative fraction was observed in this case.
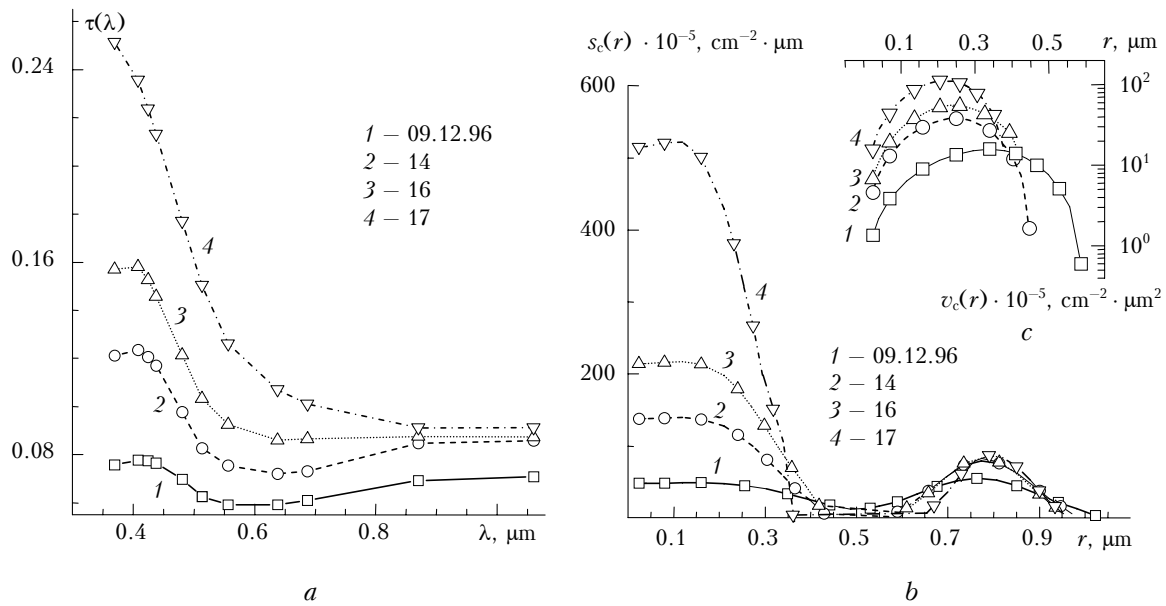
Fig. 3. Daily mean spectra of AOT (*a*), size distributions of geometric cross section $s_c(r)$ (*b*), and dynamics of the accumulative fraction (*c*) along the route approaching the Europe (September 12–17, 1996).
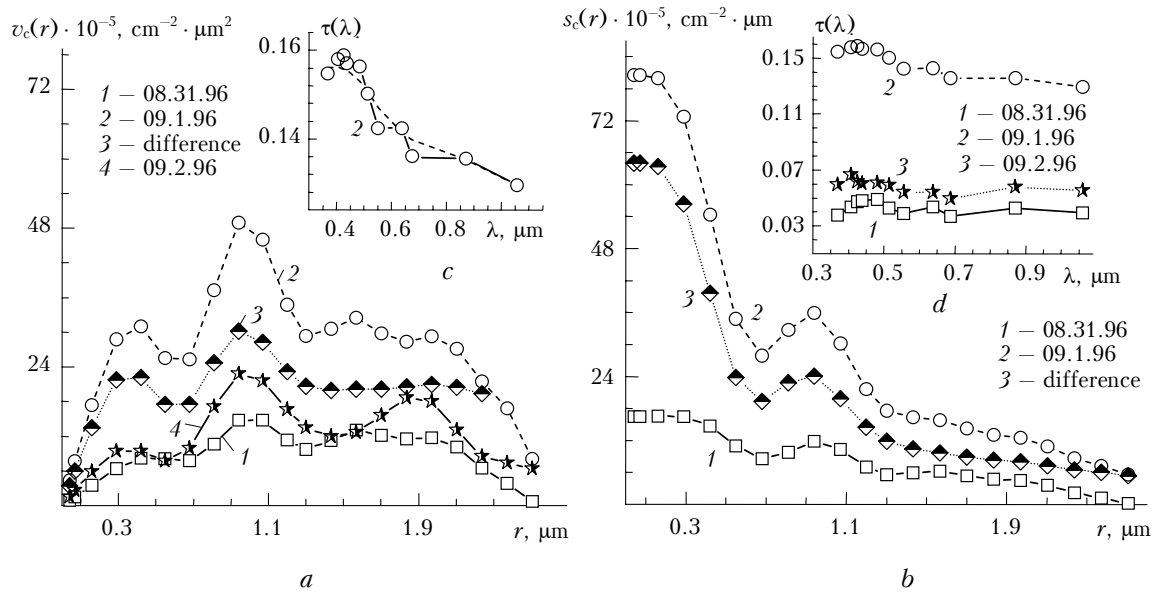

Fig. 4. Size distributions of particle volume $v_c(r)$ (*a*) reconstructed from daily mean spectra of AOT (*d*), dynamics of the distribution $s_c(r)$ (*b*), comparison of the calculated $\tau(\lambda)$ (dashed line) with measured (*c*). Curve *3* in Fig. 4*a* is calculated as the difference between curves *1* and *2*.

Table 2. Estimates of the integral parameters of the particle size distributions in different size ranges obtained by inverting $\tau(\lambda)$ (Figs. 4*c* and *d*)

Date	Fraction								
	$r < 0.5\ \mu m$			$0.5 < r < 1.2\ \mu m$			$r > 1.2\ \mu m$		
	$V_a \cdot 10^{-5}$, $\mu m^3 \cdot cm^{-2}$	$S_a \cdot 10^{-5}$, $\mu m^2 \cdot cm^{-2}$	$r^a_{,eff}$, μm	$V_i \cdot 10^{-5}$, $\mu m^3 \cdot cm^{-2}$	$S_i \cdot 10^{-5}$, $\mu m^2 \cdot cm^{-2}$	$r^i_{,eff}$, μm	$V_c \cdot 10^{-5}$, $\mu m^3 \cdot cm^{-2}$	$S_c \cdot 10^{-5}$, $\mu m^2 \cdot cm^{-2}$	$r^c_{,eff}$, μm
08.31.96	3	43	0.21	8	29	0.81	11	21	1.58
09.1.96	12	181	0.19	23	87	0.80	39	70	1.68
09.2.96	4	60	0.19	11	40	0.82	17	31	1.67

The results of solution of the inverse problem are shown in Figs. 5a and b, where dotted line (curve 4) indicates the difference between the size spectra of aerosol before and after the peak of AOT values. It is seen from the data presented that no essential changes are observed in the size range of the intermediate fraction.
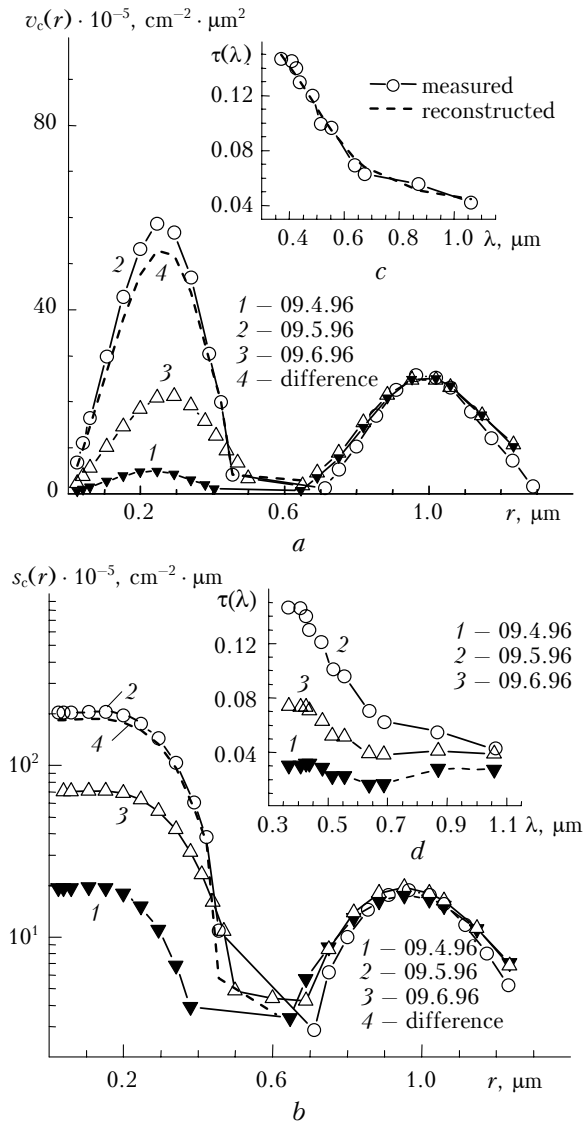

Fig. 5. Distributions $v_c(r)$ reconstructed from individual realizations $\tau(\lambda)$ [$k = 64$; 69; 74 (d)] (a), dynamics of the distribution $s_c(r)$ (b), comparison of the calculated and measured data (c).

It should be emphasized that on September 4, 1996, quite low levels of the content of accumulative fraction in the atmospheric column were observed before first and second peaks of $\tau(\lambda)$: $V_a \sim 3.0 \cdot 10^{-5} \ \mu m^3 \cdot cm^{-2}$. We have managed to estimate the relative contributions of both fractions to the extinction of optical radiation from solution of the inverse problem. These estimates show (Fig. 6a) that the optical effect of accumulative fraction can decrease down to the level at which the contribution

of intermediate fraction becomes prevalent practically in the entire wavelength range. The characteristic size of particles of intermediate fraction over the ocean is a little bit greater (Fig. 6b) than that over the continent.[4] Let us also note that, apart from very low content of particles of accumulative fraction over the ocean, its right-hand boundary is shifted to smaller size, that it is observed over the continent. The obtained estimates of the right-hand boundary of accumulative fraction agree with the analogous estimates presented in Ref. 5.
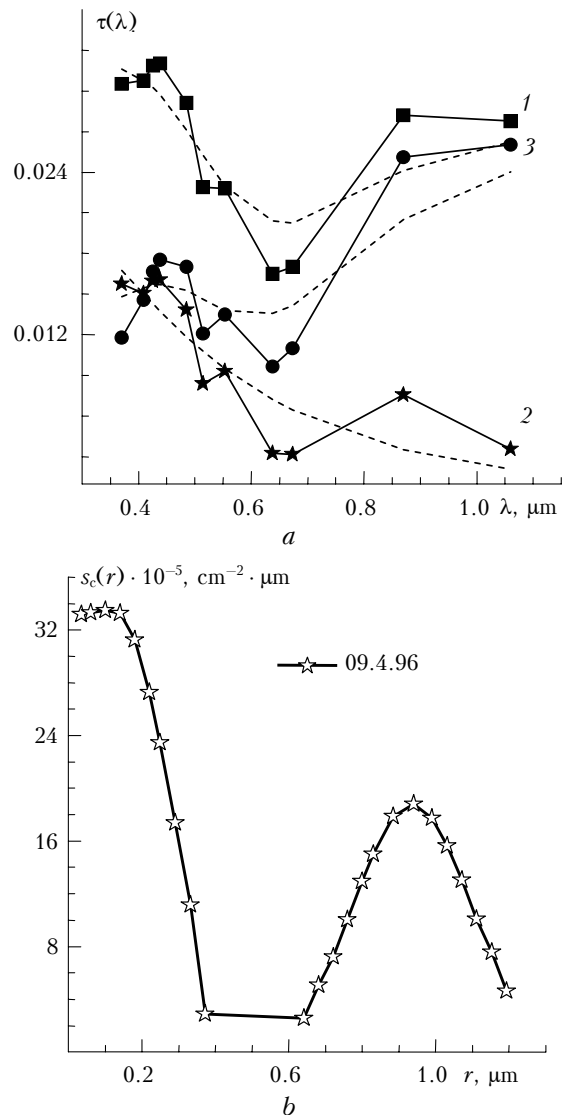

Fig. 6. Optical contributions of accumulative (2) and intermediate (3) fractions to measured $\tau(\lambda)$ values (1) from the data measured on September 4, 1996 (a) and reconstructed distribution $s_c(r)$ (b). Dashed lines show smoothed spectral dependences of the AOT.

To analyze the disperse composition of marine aerosol (without the effect of continental sources), the realizations $\tau_k(\lambda)$ obtained in the regions near continents ($k = 1–20$ and $125–163$) were excluded from the total data array, as well as the data

obtained during the period of two peaks of the atmospheric turbidity (k = 30–40 and 64–85) also caused by emissions of the continental aerosol. Weak correlation of the values $\tau(\lambda_i)$ with relative humidity in the near-surface layer is characteristic of thus formed data array (OO, background) (ρ_{cor} = –0.02), and, at the same time, optical data show noticeable correlation with the wind velocity S_w in the near-water layer (the correlation coefficient ρ_{cor} is approximately –0.31).

The nonlinear dependence of $\tau(\lambda)$ on wind velocity was revealed earlier[1] in analyzing the effect of meteorological conditions on the aerosol turbidity. Analogous analysis carried out for the ensemble of "OO, background" realizations (Fig. 7) has shown the presence of the aforementioned correlation at all wavelengths (lines in Fig. 7 show the moving average). The nonlinear dependence of the atmospheric transparency on wind velocity was also observed earlier[6] in measurements of the spectral transmission of the atmosphere on the near-ground paths in a coastal zone of the Black Sea.

The efficiency of filling of the atmospheric column with particles of marine aerosol depends not only on the intensity of their generation by ocean surface, but also on the regime of turbulent mixing in the near-water layer providing vertical transfer as well as on the ratio of the thermal and dynamic components and on the state of stable stratification. Two types of air flows are usually selected over the sea surface due to relatively small values of the roughness parameter (at low waves): aerodynamic

smoothed (at the values of the parameter $u_* z_0 / \nu$ < 0.13) and turbulent (at $u_* z_0 / \nu$ > 2.5).[7,8] Here u_* is the wind speed scale (friction speed); z_0 is the roughness scale of the underlying surface, ν is the viscosity of the air.

As wind velocity over the ocean surface increases, the values characterizing the magnitude of the numerator of the parameter change, and the regime of turbulent mixing (due to the dynamic component) gradually varies from aerodynamic smoothed flow (through the transition zone) to the turbulent one. The height of the mixing layer changes depending on the ratio of the dynamic and convective components of the regime of turbulent mixing, then the efficiency of filling of the atmospheric column with aerosol particles emitted from the sea surface changes.

It is seen from Fig. 7 that, as the wind velocity increases from calm to 3 m/s, the intensity of emission of aerosol particles to the atmosphere increases, because the thermal component (on latitudes under consideration) at the given values S_w remains prevalent over the dynamic component. As the dynamic component intensifies, the turbulent diffusion coefficient increases, that leads to an increase in the efficiency of sink of aerosol particles due to the increase of the so-called effective velocity of "dry deposition" to the water surface. So, the maximum of efficiency of filling the atmospheric column with particles generated on the water surface, mainly by the "bubble mechanism,"[3] is reached at the S_w values of 2 to 3 m/s.
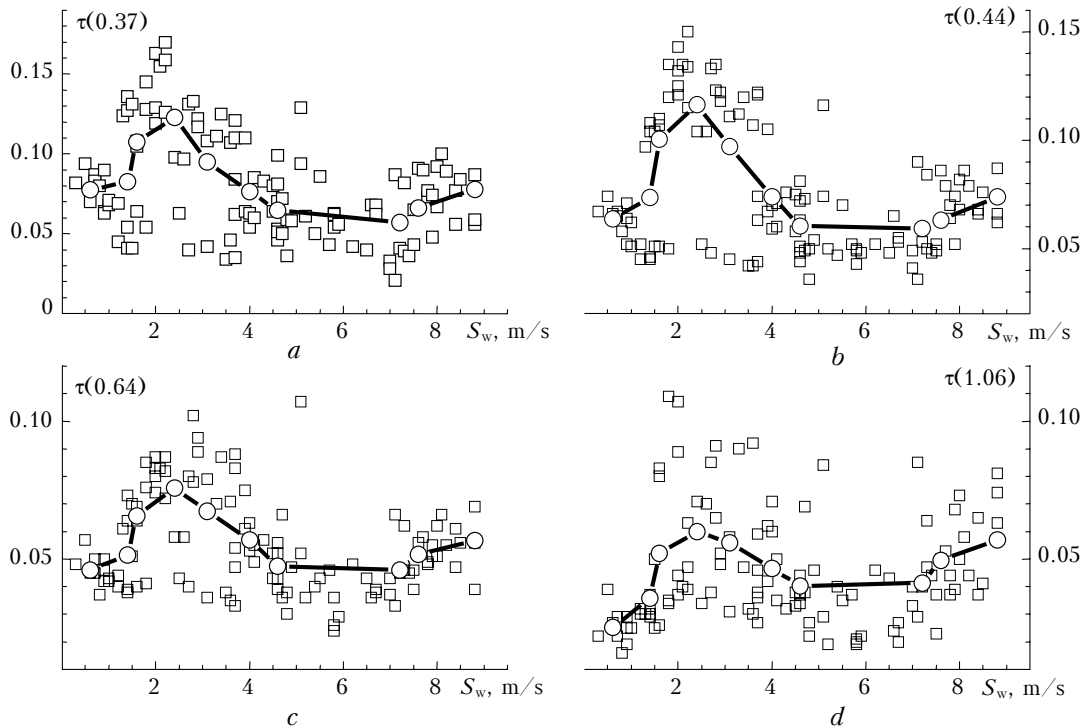

Fig. 7. The change of $\tau(\lambda)$ with the increasing wind velocity.

The efficiency of aerosol generation by the ocean surface increases at the values of wind velocity greater than 5–6 m/s due to the additional mechanism − blowing off of the splashes from ridges of the broken waves, which determines the next stage of the increase of the aerosol content in the atmospheric column. Thus, as is seen in the data presented in Fig. 7, the observed variations of the spectral dependences of AOT (Fig. 8) are characterized by the change of three stages of their transformation as wind velocity increases.
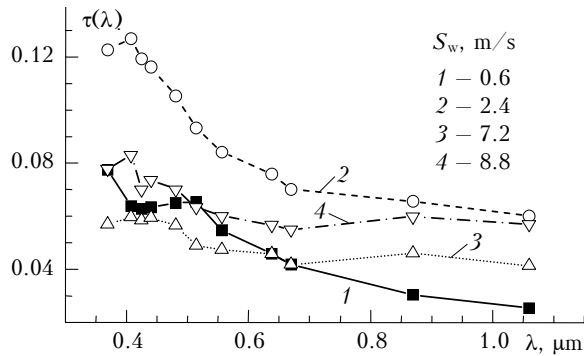

Fig. 8. The change of the shape of the spectral dependence of AOT as a function of wind velocity.

It should be also noted that, as wind velocity increases, the efficiency of drying of the emitted particles also increases, that decreases the efficiency of sedimentation of heavy particles to the water surface. All the abovementioned circumstances, to a

significant degree, cause the transformation of the aerosol particle size spectrum with the wind velocity increase considered below.

The mean spectral dependences $\tau(\lambda)$ for the set of values of wind velocity S_w from calm 0.6 to high 9 m/s were calculated from the data obtained as moving average (Fig. 8, Table 3). No higher wind velocities were considered because of a short statistics of the experimental data.

The particle volume size distributions were reconstructed separately for three ranges of wind velocity or three stages of its variability (Fig. 9) on the basis of averaged spectra of AOT presented in Table 3.

Stable increase of the content of particles of both accumulative and intermediately dispersed fraction occurs on the first stage. Then the stage of the decrease of the concentration of particles is observed, which is better pronounced for accumulative fraction. As a certain level has been reached, the content of fine particles already does not change.

Another situation is observed in the dynamics of intermediately dispersed fraction. Starting from wind velocity of ~ 4.6 m/s the increase of its content is observed caused by intensification of aerosol generation by water surface due to the increase of the dynamic component of the regime of turbulent mixing and the aforementioned mechanism of blowing off the splashes from ridges of broken waves. Thus, particles of intermediately dispersed fraction are more effectively emitted to the atmospheric column over ocean.

Table 3. The change of averaged measured $\tau(\lambda)$ values as functions of wind velocity

| λ, μm	S_w, m/s									
	0.6	1.4	1.6	2.4	3.1	4.0	4.6	7.2	7.6	8.8
0.369	0.077	0.082	0.108	0.123	0.095	0.076	0.065	0.057	0.066	0.078
0.408	0.064	0.075	0.106	0.127	0.103	0.080	0.063	0.060	0.069	0.083
0.425	0.063	0.072	0.099	0.119	0.096	0.075	0.061	0.059	0.064	0.070
0.44	0.064	0.074	0.100	0.116	0.097	0.074	0.060	0.059	0.063	0.074
0.481	0.065	0.070	0.091	0.105	0.087	0.071	0.060	0.056	0.063	0.070
0.514	0.065	0.067	0.083	0.093	0.076	0.066	0.057	0.049	0.055	0.063
0.556	0.055	0.059	0.074	0.084	0.072	0.061	0.052	0.047	0.053	0.060
0.638	0.046	0.052	0.066	0.076	0.067	0.057	0.047	0.046	0.052	0.057
0.67	0.042	0.046	0.061	0.070	0.061	0.051	0.043	0.042	0.048	0.055
0.87	0.030	0.041	0.058	0.066	0.060	0.052	0.044	0.046	0.054	0.060
1.06	0.025	0.036	0.052	0.060	0.056	0.047	0.040	0.041	0.049	0.057
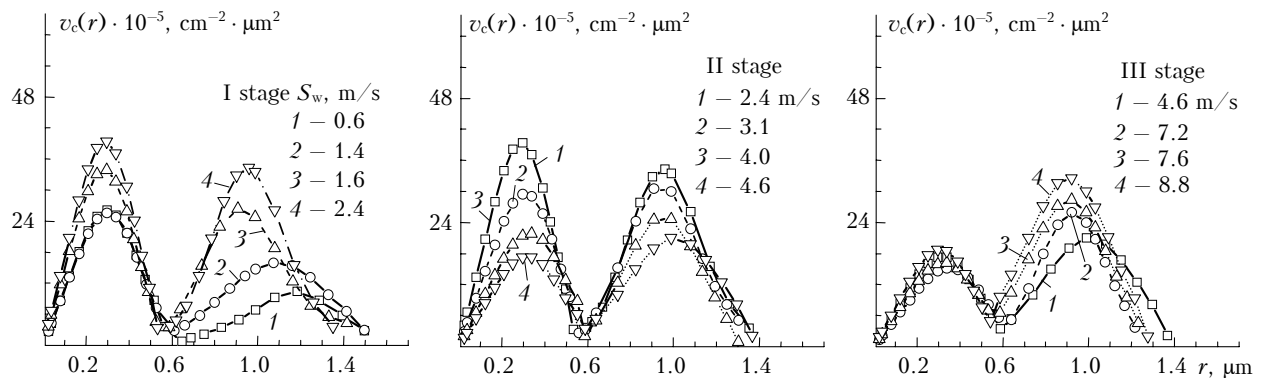
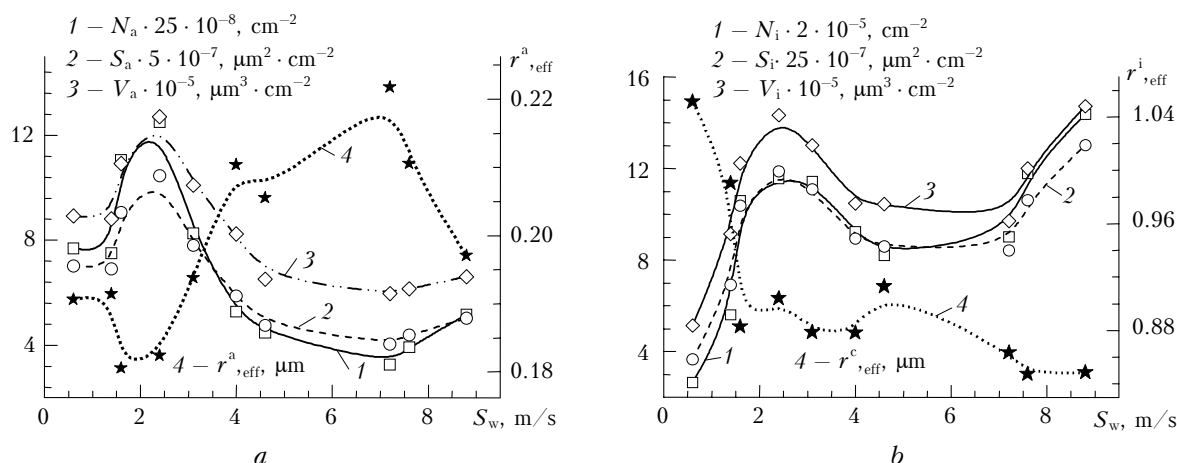**Fig. 9.** Dynamics of variations of the particle volume size distributions as a function of wind velocity.

Fig. 10. Dynamics of variations of the parameters of the size spectrum N, S, V, and the effective size r_{eff} of aerosols of accumulative (*a*) and intermediate (*b*) fractions.

Table 4. The change of the integral parameters of size distributions of particles of accumulative and intermediate fractions as functions of the wind velocity

S_w, m/s	Accumulative				Intermediately dispersed			
	$N_a \cdot 10^{-5}$, cm^{-2}	$S_a \cdot 10^{-5}$, $\mu\text{m}^2 \cdot \text{cm}^{-2}$	$V_a \cdot 10^{-5}$, $\mu\text{m}^3 \cdot \text{cm}^{-2}$	$r^a_{,\text{eff}}$, μm	$N_i \cdot 10^{-5}$, cm^{-2}	$S_i \cdot 10^{-5}$, $\mu\text{m}^2 \cdot \text{cm}^{-2}$	$V_i \cdot 10^{-5}$, $\mu\text{m}^3 \cdot \text{cm}^{-2}$	$r^i_{,\text{eff}}$, μm
0.6	308	140	8.9	0.19	1.1	14.7	5.1	1.05
1.4	300	138	8.8	0.19	2.2	27.6	9.1	0.99
1.6	443	181	10.9	0.18	4.2	41.5	12.2	0.88
2.4	500	209	12.7	0.18	4.6	47.5	14.3	0.90
3.1	331	156	10.1	0.19	4.6	44.4	13.0	0.88
4.0	211	117	8.2	0.21	3.7	35.7	10.5	0.88
4.6	179	95	6.5	0.21	3.3	34.3	10.4	0.91
7.2	130	81	6.0	0.22	3.6	33.7	9.7	0.86
7.6	157	88	6.1	0.21	4.7	42.5	12.0	0.85
8.8	206	101	6.6	0.20	5.7	52.0	14.7	0.85

Mutual dynamics of the changes of the integral signs (total cross section, volume, and number density) is shown in Fig. 10. The values of the signs are reduced to the same scale using the factors indicated in notations of curves in Fig. 10. Convergent dynamics of the change of the effective size of particles of the analyzed fractions (curves *4*) attracts our attention. The specific values of the parameters shown in Fig. 10 are presented in Table 4.

Conclusion

Summarizing the results obtained, let us note that those confirm the principal conclusions[1,2] and show that the most essential variations of the disperse composition of the aerosol component over the ocean are caused, first of all, by the transfer of continental aerosol by different types of air masses. The results of inversion show that the effect of continent on the microstructure of the aerosol component in mid-latitudes of the Atlantic is observed at a significant distance from continents, ~ 500 km and more. As moving from continents, the content of accumulative fraction decreases almost by an order of magnitude. Over the open ocean, except for some episodes of disturbed AOT, optical

contribution of large particles ($r > 0.45$ μm) undergoes small oscillations, but is practically equal and often exceeds the optical effect of accumulative fraction.

Analysis of the spectral AOT measured during the passage of air masses enriched with aerosols of continental origin has shown that the increase of content of accumulative fraction is usually observed. However, in some cases at changes of air masses we observed essential disturbances of the aerosol disperse composition in the size range of intermediate and coarse fractions with $r > 0.4$ μm. The observed differences in the aerosol disperse composition are caused by different trajectories of the motion of air masses – at long stay of continental air over ocean the enhanced level of the content of accumulative fraction is observed longer than that of large aerosol particles.

Analysis of the dependence of the characteristics of marine aerosol on wind velocity has shown that one can select three stages in transformation of the disperse composition. At the first stage (wind velocity up to ~ 2.4 m/s), stable increase of the contents of both accumulative and intermediate fractions occurs. Then (in the range $S_w = 2.4$–4.6 m/s) the stage of stabilization and some decrease

of the concentration of particles are observed. As some minimum level has been reached, the content of accumulative fraction already does not change.

Another sequence is observed in the dynamics of variations of the intermediate fraction. Starting from the wind speed of 4 to 5 m/s, the content of particles increases again. The reason is intensification of the dynamic component of the regime of turbulent mixing and the effect of the mechanism of blowing off of splashes from the wave crests. Thus, at high winds, particles of intermediate fraction are more effectively emitted to the atmospheric column from the ocean surface. It is worthy to note that some peculiarities in the behavior of the disperse structure of atmospheric haze that were noted as the wind strengthened are not universal. Those only reflect the specific features of the optical data obtained during this research mission. Actually further investigations are needed, but in a wider wavelength range.

Acknowledgments

References

1. S.M. Sakerin and D.M. Kabanov, Atmos. Oceanic Opt. **12**, No. 2, 93–98 (1999).
2. E.V. Makienko, D.M. Kabanov, R.F. Rakhimov, and S.M. Sakerin, Atmos. Oceanic Opt. **17**, Nos. 5–6, 387–392 (2004).
3. K.Ya. Kondratyev and D.V. Pozdnyakov, *Aerosol Models of the Atmosphere* (Nauka, Moscow, 1981), 103 pp.
4. E.V. Makienko, R.F. Rakhimov, S.M. Sakerin, and D.M. Kabanov, Atmos. Oceanic Opt. **15**, No. 7, 531–540 (2002).
5. A. Smirnov, B.N. Holben, Y.J. Kaufman, O. Dubovik, T.F. Eck, I. Slutsker, C. Pietras, and R.N. Halthore, J. Atmos. Sci. **59**, No. 3, Part. 1, 501–502 (2002).
6. M.V. Kabanov, M.V. Panchenko, Yu.A. Pkhalagov, V.V. Veretennikov, V.N. Uzhegov, and V.Ya. Fadeev, *Optical Properties of Coastal Atmospheric Hazes* (Nauka, Novosibirsk, 1988), 202 pp.
7. A. Goroch, S. Burk, and K.L. Davidson, Tellus **32**, No. 3, 245–250 (1980).
8. V.F. Derr, *Remote Sensing of Troposphere* (WPL ERL EED, Boulder, Colorado, 1972), 854 pp.